Supporting Information

Amorphous Tin-based Nanohybrid for Ultra-Stable Sodium Storage

Zhongtao Li,[a] Jianze Feng,[a] Han Hu,[a] Yunfa Dong,[a] Hao Ren,[a] Wenting Wu,[a] Zhenpeng Hu,[b]* and Mingbo Wu[a]**

a. State Key Laboratory of Heavy Oil Processing, College of Chemical Engineering, China University of Petroleum (East China), Qingdao 266580, P. R. China.

b. School of Physics, Nankai University, Tianjin 300071, P. R. China.

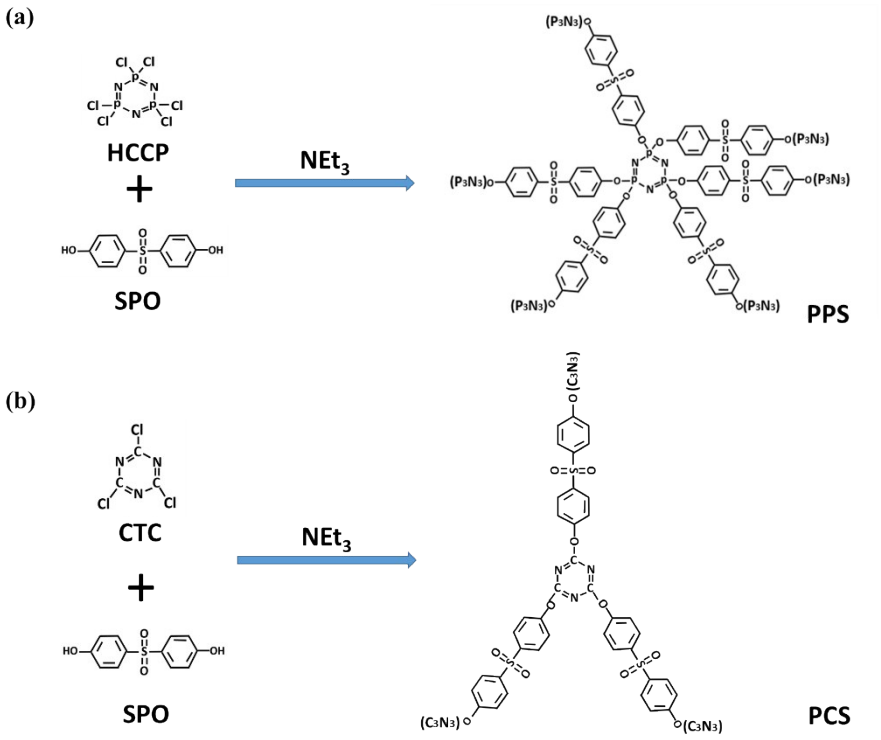

Fig. S1 a) A polymerization of hexachlorocyclophosphazene and 4, 4'-sulfonyldiphenol to obtain a supermolecule polymer of poly(cyclotriphosphazene-co-4,4’-sulfonyldiphenol) (PPS). b) A polymerization of cyanuric chloride and 4, 4'-sulfonyldiphenol to obtain a supermolecule polymer of poly(cyanuric-co-4,4’-sulfonyldiphenol) (PCS).

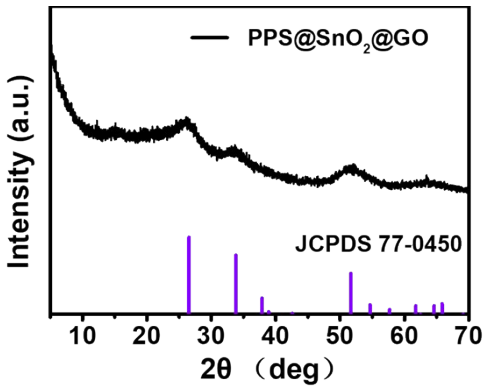

Fig. S2 a) XRD patterns of PPS@SnO_2@GO.

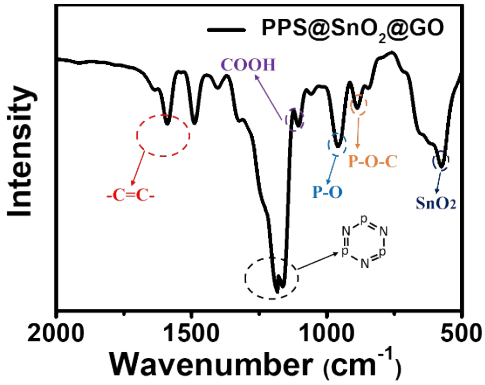

Fig. S3 FT-IR spectra of PPS@SnO_2@GO.

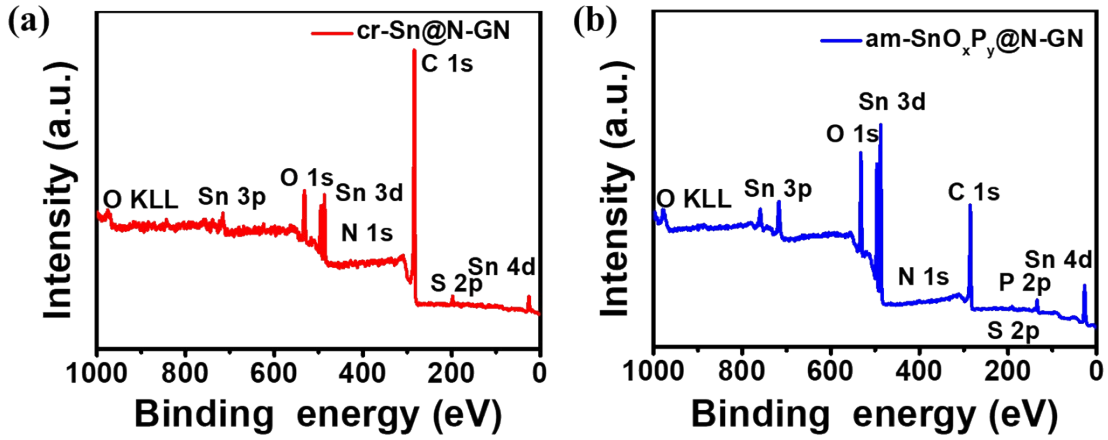

Fig. S4 a) XPS survey spectrum of am-SnO_xP_y@N-GN. b) XPS survey spectrum of cr-Sn@N-GN.

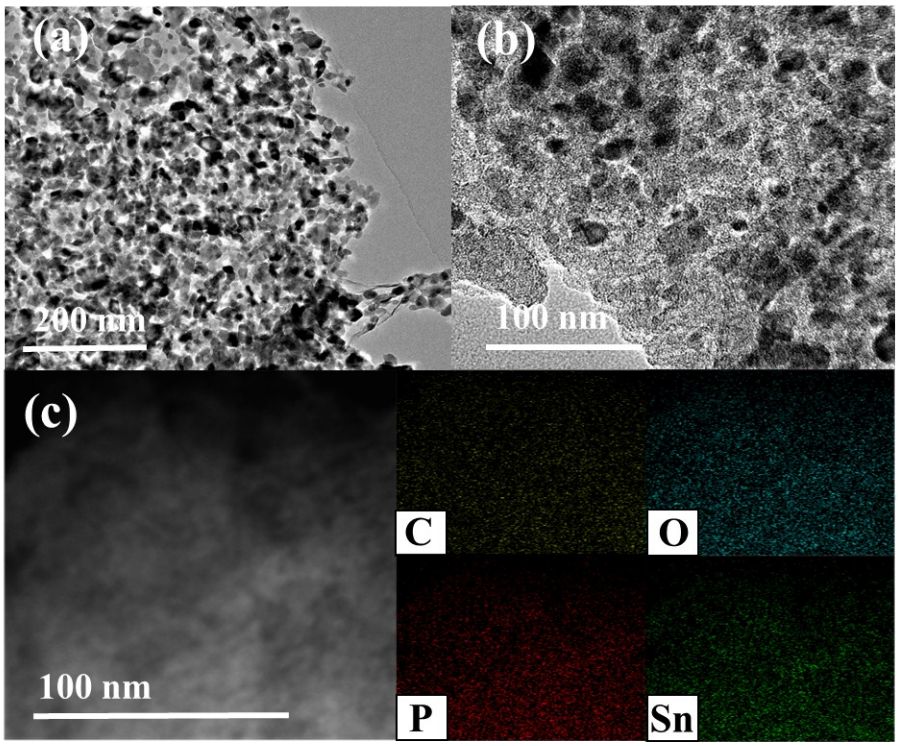

Fig. S5 a) TEM images of cr-Sn@GN architecture. b) TEM images of PPS@SnO_2@GO architecture. b) EDS mapping image of am-SnO_xP_y@N-GN (up-left: C-K mapping, up right: O-K mapping, bottom-left: P-K mapping, bottom-right: Sn-K mapping).

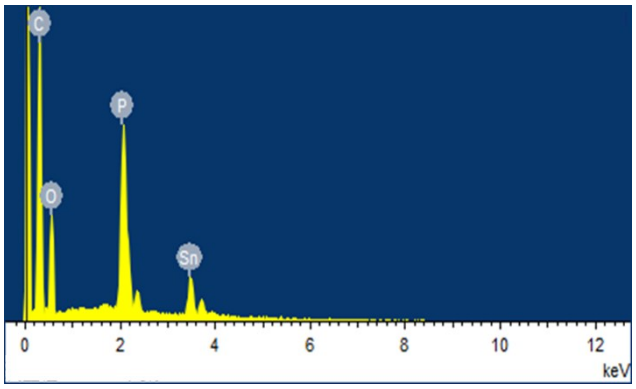

Fig. S6 EDS spectra elemental analysis of am-SnO_xP_y@N-GN.

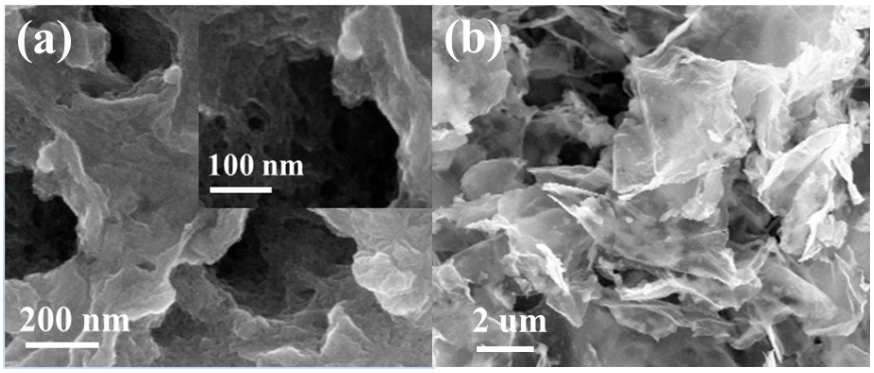

Fig.S7 a) SEM images of am-SnO_xP_y@N-GN architecture. b) SEM images of cr-Sn@GN architecture.

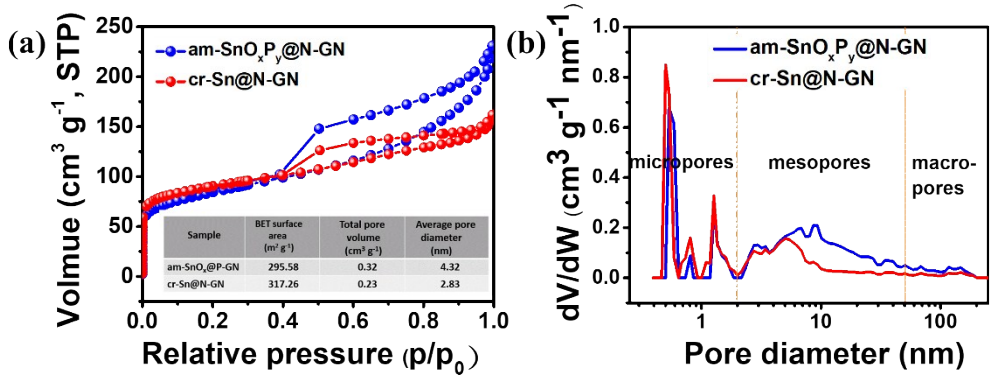

Fig. S8 a) N_2 adsorption/desorption isotherm of am-SnO_xP_y@N-GN and cr-Sn@N-GN architecture. b) The corresponding pore distribution curves (BJH method).

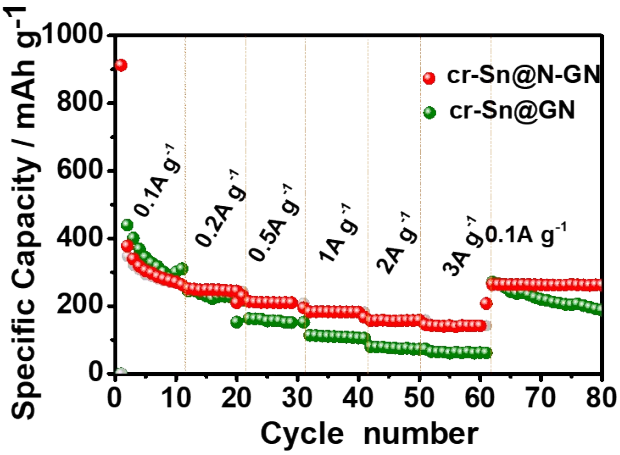

Fig. S9 Rate capabilities of cr-Sn@N-GN and cr-Sn@GN.

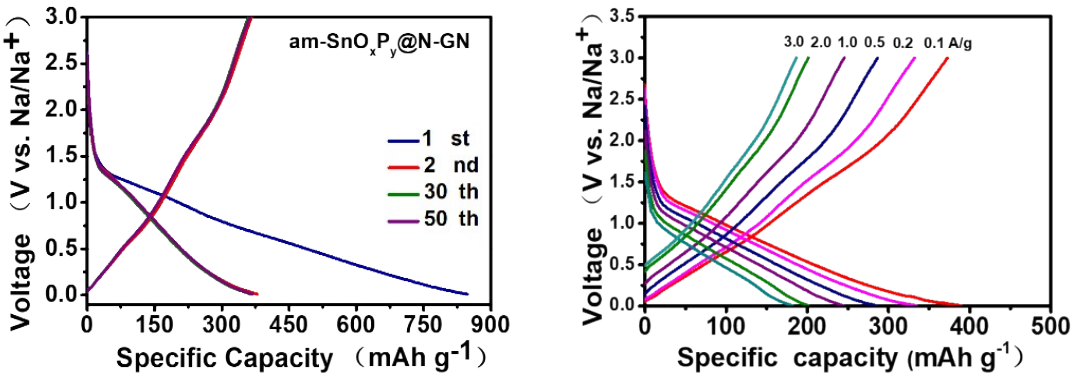

Fig. S10 a) Galvanostatic discharge-charge profiles of the am-SnO_xP_y@N-GN at 100 mA g^{-1}. b) Galvanostatic discharge-charge profiles of the am-SnO_xP_y@N-GN from 100 mA g^{-1} to 3000 mA g^{-1}.

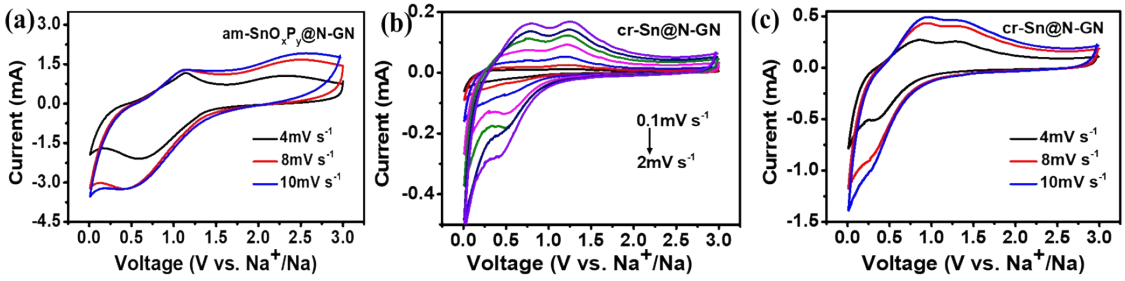

Fig. S11 a) CV curves of am-SnO_xP_y@N-GN at various sweep rates from 4 to 10 mV s^{-1}. b) CV curves of cr-Sn@N-GN at various sweep rates from 0.1 to2 mV s^{-1}. b) CV curves of cr-Sn@N-GN at various sweep rates from 4 to10 mV s^{-1}.

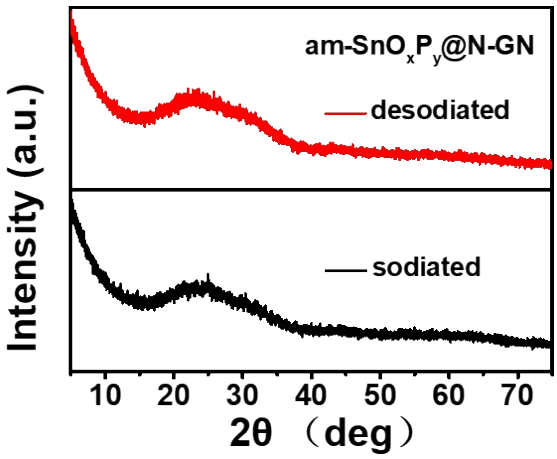

Figure. S12 XRD spectra of the am-SnO_xP_y@N-GN electrode at different stages.

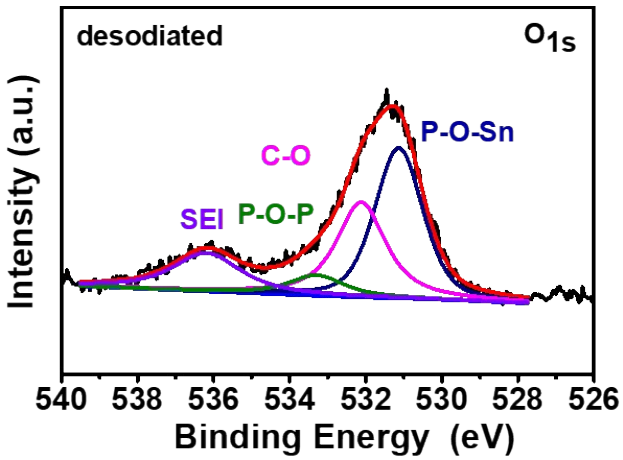

Fig. S13 Chemical composition analysis though XPS of O for am-SnO_xP_y@N-GN.

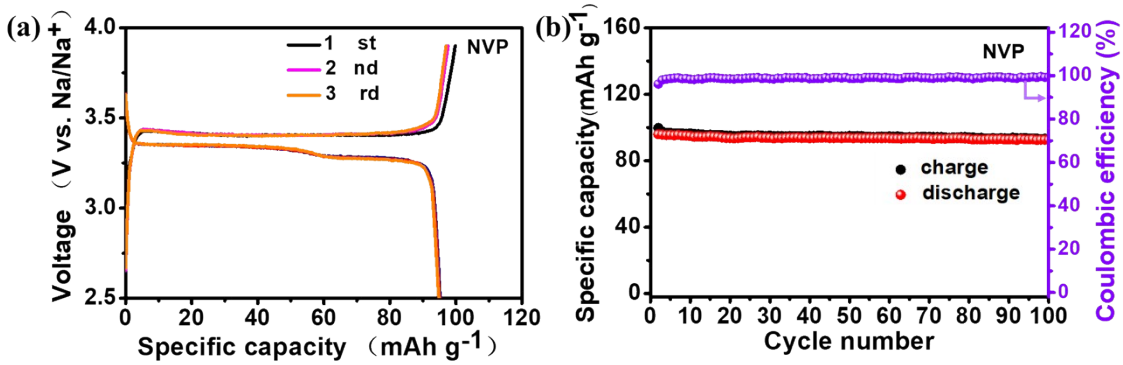

Fig. S14 a, b) Electrochemical performance of $Na_3V_2(PO_4)_3$/C (NVP) cathode. a) charge/discharge curves of the NVP cathode at 1C (1C =118 mA h g^{-1}). b) cycling performance of the $Na_3V_2(PO_4)_3$/C (NVP) cathode at 1C.

Table S1 ICP-OES and EDS spectra elemental analysis

	Sn	P	O
ICP (wt%)	45	n/a	n/a
EDS (wt%)	18.4	12.2	18.8
EDS (at%)	1	2.4	7.5

Table S2. The Comparison of the Electrochemical Properties for the am-SnO_xP_y@N-GN and Other Works in Coin Cell Configuration.

Sample	Cycling stability			Rate capacity			Re
	Current density [mA g^{-1}]	Capacity after cycles [mAh g^{-1}]	C.N (capacity retention(%))	Current density [mA g^{-1}] (Capacity [mAh g^{-1}])			
am-SnO_xP_y@N-GN	1000	201.6	3000(74.4%)	100(378)	1000(267)	6000(78)	☑
Yolk−Shell Sn@C	1000	200	1000(40.0%)	200(450)	1000(320)	5000(200)	1
Mesoporous SnO_2	180	200	500(21.0%)	120(800)	660(560)	1320(450)	2
SnO_2/CNT-SCO_2	50	230	100(83.3%)	20(500)	500(280)	1000(220)	3
Sn/SnO_2/C	100	300	100(66.6%)	100(282)	500(280)	1000(120)	4
SnO_2-PC	100	281	250(98.1%)	100(310)	1600(107)	3200(80)	5
SnO_2 /GO	113	245	150(55.8%)	50(480)	500(196)	1000(125)	6
$Sn_2Nb_2O_7$/SnO_2	100	300	100(81.1%)	100(302)	1000(202)	5000(135)	7
SnO_2/3D-RGO	50	223	350(53.6%)	80(321)	800(276)	1200(266)	8
cactus-like SnO_2	50	500	50(65.5%)	180(312)	540(276)	3200(130)	9

Cycle number denoted as C.N. ☑ Represents our work. Capacity retention calculated from the first charge capacity

1. S. Li, Z. Wang, J. Liu, L. Yang, Y. Guo, L. Cheng, M. Lei and W. Wang, *ACS Appl Mater Interfaces*, 2016, **8**, 19438-19445.
2. H. Bian, R. Dong, Q. Shao, S. Wang, M. Yuen, Z. Zhang, D. Yu, W. Zhang, J. Lu and Y. Li, *J. Mater. Chem. A*, 2017, **5**, 23967-23975.
3. J. Patra, H. Chen, C. Yang, C. Hsieh, C. Su and J. Chang, *Nano Energy*, 2016, **28**, 124-134.
4. Y. Cheng, J. Huang, J. Li, Z. Xu, L. Cao and H. Qi, *J. Pow. Sour*, 2016, **324,** 447-454.
5. Z. Huang, H. Hou, G. Zou, J. Chen, Y. Zhang, H. Liao, S. Li and X. Ji, Electrochimica Acta, 2016, **214,** 156-164.
6. Y. Wang, Y. Lim, M. Park, S. Chou, J. Kim, H. Liu, S. Dou and Y. Kim, *J. Mater. Chem. A*, 2014, **2**, 529-534.
7. P. Zhai, J. Qin, L. Guo, N. Zhao, C. Shi, E. Liu, F. He, L. Ma, J. Li and C. He, *J. Mater. Chem. A*, 2017, **5**, 13052-13061.
8. J, Lee, J. Song, Y. Cha, S. Fu, C. Zhu, X. Li, Y. Lin and M. Song, Nano Res, 2017, **10,** 4398-4414.
9. Z. Huang, H. Hou, G. Zou, J. Chen, Y. Zhang, H. Liao, S. Li and X. Ji, *Electrochimica Acta*, 2016, **214**, 156-164.